Results in Engineering 24 (2024) 103194

Contents lists available at ScienceDirect

Results in Engineering

journal homepage: www.sciencedirect.com/journal/results-in-engineering

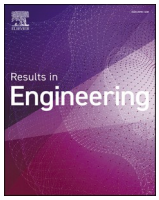

Review article

# Metallic cutting inserts fabrication by means of additive manufacturing with fused filament fabrication technology

Francisco Martín-Fernández [a], María Jesús Martín-Sánchez [a,*], Guillermo Guerrero-Vacas [b], Óscar Rodríguez-Alabanda [b]

[a] Department of Civil, Materials and Manufacturing Engineering, University of Malaga. Málaga 29071, Spain
[b] Department of Mechanics, University of Córdoba, Córdoba 14071, Spain

ARTICLE INFO

*Keywords:*
Cutting tool
Additive manufacturing
H13 tool steel
EN AWS-2030 aluminium
Finish surface

ABSTRACT

The present work developed a first approach to the manufacturing of turning inserts using the emerging Additive Manufacturing (AM) technology, specifically employing the fused filament fabrication (FFF) process, based on the extrusion of material and deposition layer by layer. Traditionally, this type of cutting tools were manufactured by powder metallurgy and machining processes, but in this instance Additive Manufacturing processes allowed the customisation of the geometries and eliminated the need of dies to manufacture these tools, leading to economic savings. The study analysed, from different perspectives, the viability of these interchangeable inserts as cutting tools. These approaches included qualitative studies of chip formation and cutting-edge wear as well as thermal and roughness analysis of specimens tested under different conditions. The behaviour of H13 Tool Steel cutting inserts on cylindrical specimens of EN AW-2030 aluminium alloy was compared with commercial carbide inserts, being observed that the chip types produced were extremely similar between those obtained by commercial and those from Additive Manufacturing, particularly in dry conditions. The qualitative study of insert wear showed that AM inserts presented overall larger contribution of built-up edge (BUE) and plastic deformation of the tip, with greater incidence at cutting speeds of Vc = 60 m/min and feed rate of fz = 0.1 mm/r. Regarding thermal analysis, the AM inserts revealed a slightly more abrasive behaviour, resulting in a temperature increase throughout the machining process of approximately 70 °C, with no significant influence from the increase in cutting speed. The study of the surface finish offered average roughness results (Ra) of 0.58 μm for commercial inserts, 1.78 μm in AM inserts with dry tests and 2.06 μm in this same type of insert but tested with lubrication. These variations in average roughness were not significant.

## 1. Introduction

Conventional mechanical manufacturing processes such as machining and, specifically, chip removal, are traditionally a fundamental option in the forming of parts, in particular on metallic alloys. The great development of this subtractive technology over the years has generated a large number of studies in which all kinds of parameters are considered, such as thermal effects, lubrication and wear conditions as well as studies of roughness and materials for machining and cutting tools fabrication, among others. In relation to these last ones (cutting tools), their manufacture has evolved from the original HSS blank bar to the current interchangeable inserts in different materials (with or without coating) mounted on the body of the tool. They are mainly produced by powder metallurgy processes in specialised industries, offering a catalogue with a wide range of different configurations, materials, coatings, etc.

The recent incorporation of a disruptive technology such as Additive Manufacturing has modified the manufacturing paradigm of functional mechanical parts and essential elements in any forming process. This includes tooling and all types of accessories, as well as cutting tools in the form of inserts, which is the focus of this article. In this context, Additive Manufacturing provides an alternative of great interest, mainly due to its capacity for customisation and adaptation to functional requirements, both geometric and material, making it a notably attractive option in fields of considerable technological interest such as aeronautics, defence, or naval, among others.

As mentioned above, tools or inserts conventionally created by powder metallurgy have been studied from many diverse approaches.

* Corresponding author.
*E-mail address:* mjmartin@uma.es (M.J. Martín-Sánchez).

https://doi.org/10.1016/j.rineng.2024.103194
Received 19 August 2024; Received in revised form 6 October 2024; Accepted 20 October 2024
Available online 4 November 2024

Thus, recently, Daniel et al. [1] address the thermal effect in H13 tool steel machining; Rall et al. [2] focus on the optimisation of turning parameters using artificial intelligence; Ab Aziz et al. [3] study the behaviour of cutting tools in Al 7075-T651 aluminium machining and Nizar et al. [4] examine the optimal surface characteristics in the machining of aluminium alloys using WC—Co cutting inserts.

In particular, the cutting tool material plays a fundamental role in a metal cutting process, either with traditional HSS (high speed steel) tools or with new materials like cemented carbide, ceramic, cermet, polycrystalline diamond or others, in a variety of different combinations in the form of inserts. In this context, Siemiatkowski et al. [5] study the durability of ceramic cutting tools made of $Cr_2O_3$; Zhang et al. [6] focus on diamond cutting tools; Pattnaik et al. [7] give attention to the machining of aluminium alloys using coated ceramic cutting tools and Ramírez et al. [8] analyse the surface finish of aluminium alloys with diamond inserts. These inserts, mostly manufactured via powder metallurgy and frequently subjected to subsequent coating processes (PVD or CVD gas deposition), are mounted in tool holders that serve to dampen the vibrations generated during the machining process.

In 1983, the emergence of the first Additive Manufacturing machine, using stereolithography (SLA) system, and the following rapid development of others multiple technologies, has opened up new lines of fabrication on all types of materials. This way, Bernatskyi [9] provide a review of the history of Additive Manufacturing in metals. Studies on stainless steels are analysed in Caminero et al. [10], Karolczuk et al. [11], Kong et al. [12], Yuan et al. [13]; Inconel is considered in Banait et al. [14], Bodner et al. [15], Wood et al. [16]; titanium by Shaikh et al. [17], Dzogbewu [18], Arjunan et al. [19]; bimetallic components in Gürol et al. [20], Rock et al. [21], Rodrigues et al. [22], Seleznev and Roy-Mayhew [23], Wu et al. [24]; multimaterial in Mussatto [25], Javed et al. [26], Dzogbewu et al. [27]; 316 L steel in Caminero et al. [28], Trojan et al. [29]; high-entropy alloys in Mahmood et al. [30], Yan et al. [31], Akinwande et al. [32]; aluminium [33]; ceramics by Yang et al. [34] and specific AM steels such as 17–4PH in Basak et al. [35], Lavecchia et al. [36].

In particular, H13 tool steel has been the subject of study by Cormier et al. [37] who described the electron beam melting (EBM) process and presented a microstructural analysis of the material. Narvan et al. [38] conducted an analysis of the residual stresses generated by fabrication through Laser Powder Bed Fusion (LPBF) technology. Trojan et al. [29] performed an analysis of the microstructure and mechanical properties of H13 Tool Steel obtained through Laser Additive Manufactured technology. In a study published in 2022 [39] examined the thermal and mechanical properties of H13 dies produced by AM using selective laser melting (SLM) and subsequent heat treatment.

In recent decades, Additive Manufacturing has developed a wide range of technologies for the production of metal components. Volpato et al. [40] examined the use of the Laser Powder Bed Fusion (LPBF) on Inconel; Wrobel et al. [41] analysed the thermal aspects of LPBF on 316 L steel; Obeidi [42] provide a guide to optimising the LPBF process in metal additive manufacturing; Mazur et al. [43] applied the Sintering Laser Melting (SLM) process on H13 tool steel and Armstrong et al. [44] offers a general view of modern metal Additive Manufacturing technologies. From an application perspective, Additive Manufacturing has expanded into virtually all sectors, as evidenced by the following references: Blakey-Milner et al. [45], Radhika et al. [46] offer respective overviews in the aerospace field, and Nayeem and Hossain [47] do the same in the automotive industry. On the other hand, there is an exponential increase in the number of works that this discipline addresses from all scopes, with studies such as those about corrosion [48] and weldability [49] on 316 L steel [49] or those [50] on compression tests [50]. Also of interest are porosity studies [51] or mechanical characterisation under vibration [52], as well as studies on residual stresses generated in electron beam melting (EBM) and selective laser melting (SLM) processes [53] or those about LPBF on H13 steel [54]. Others studies addressed rheological aspects [55], fatigue behaviour on Inconel 718 [56], impact strength on multi-materials [57] or computational studies on the prediction of mechanical properties of metallic parts [58]. Mecheter and Kucukvar [59] presents an interesting economic study of conventional processes versus Additive Manufacturing processes and Li et al. [60] and Maleki et al. [61] gave attention to the cost or finish surface respectively, both in AM parts subjected to post-processing operations.

In light of the aforementioned extensive development, Additive Manufacturing presents the potential for the production of highly customised parts in medium or small batches (even single prototypes), at a moderate cost and with mechanical behaviour compatible with functional requirements. Nevertheless, one aspect that has not been adequately addressed in this context is the cutting tool, which plays a decisive role in machining processes involving chip removal. In this particular instance, the cutting tool takes the form of an insert. A review of the literature reveals that this type of component has been studied in non-metallic materials, such as those investigated by Traxel and Bandyopadhyay [62], on diamond inserts or those formed by Stellite$^{(TM)}$ [63]. Siemiatkowski et al. [5] proposes the use of ceramic cutting tools while [64] analysed the effects of coating inserts with nickel alloy powder and Meliani et al. [65], Sykora et al. [66] investigated the influence of cemented carbide inserts on surface finish.

The number of studies developing the use of additive manufacturing for the creation of cutting tools is limited. Those that do exist are primarily focused on sintering laser melting (SLM) technologies for materials that are predominantly ceramic. In this sense, additive manufacturing with FFF technology is a more economical alternative, which also adjusts perfectly to small batch sizes (even of a single element). Moreover, these processes are perfectly applicable on metallic materials (H13 tool steel) and allow different characteristics to be obtained to the standard ones (internal cooling channels, tip customisation in shapes and dimensions, etc.). All this make them of great interest in the mechanical manufacture of cutting tools.

Considering the various approaches outlined above, this work offers a novel alternative in the manufacture of metal cutting inserts using fused filament fabrication (FFF) technology. The metallic material selected is H13 tool steel, whose qualities for cutting easy machining alloys are known. The process consists of three steps: in the first step, the metallic material, in the form of a filament (metallic powder bound in a polymeric matrix), is heated and extruded, creating the part layer by layer. The second phase corresponds to the washing process and, finally, in the third phase, the part is sintered in a furnace with a controlled atmosphere. This last phase confers similarly characteristics to the conventional manufacture of inserts by powder metallurgy, even in processes similar to the infiltration of metal in sintered parts [23]. Since the cutting insert is a functional component, it must satisfy the basic requirements demanded of it in machining processes, so the aim of this first approach is to establish a range of optimal conditions for its use as

**Table 1**
EN AW 2030. Chemical composition. ISO 209:2007.

| Si | Fe | Cu | Mn | Mg | Cr | Zn | Other elements | Ti | Other non specific elements | | Al |
|---|---|---|---|---|---|---|---|---|---|---|---|
| | | | | | | | | | Each | Total | |
| 0.8 | 0.7 | 3.3–4.5 | 0.20–1.0 | 0.50–1.30 | 0.1 | 0.5 | 0.20 Bi, 0.8–1.5 Pb | 0.2 | 0.1 | 0.3 | rest |

**Table 2**
EN AW 2030. Mechanical properties (Font: ACP Materials S.L.).

| Elastic Modulus [GPa] | Yield Strength (MPa) | Tensile Strength (MPa) | Elongation at 5.65 % | Hardness (Brinell) | Density (kg/m$^3$) |
|---|---|---|---|---|---|
| 72 | 360 | 460 | 11 | 115 | 2820 |

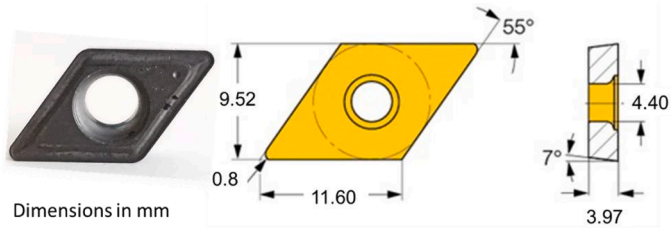


**Fig. 1.** Cutting insert DCMT 11T308–14 IC20. Manufacturer ISCAR.

well as to analyse the effect generated on the inserts by the different cutting conditions, identifying the evolution of the temperature in the cutting zone and the wear caused on these cutting tools. All of this in order to determine their useful life [67]. This technology generates fully functional inserts, making it one of the most suitable alternatives for the production of customised solutions for machining processes with the advantages of Additive Manufacturing.

## 2. Materials and methods

### 2.1. Material of the part to be machined

The use of aluminium alloys, and other light alloys, is of real interest in the aeronautical industry, as well as in all those fields where the strength/weight ratio is fundamental in the fabrication of components. In this case, due to its high machinability index, the aluminium alloy AlCu4PbMg EN AW-2030 (ISO, 2007) (Tables 1 and 2) has been chosen as test material in the turning of specimens to determine the mechanical behaviour of cutting inserts manufactured by Additive Manufacturing. Different aspects have been taken into consideration in this technical viability study, such as the level of wear and its influence on the surface finish grade, or the influence of the cutting parameters on the aluminium machining.

### 2.2. Cutting insert materials

Commercial inserts were used in the study with the objective of serving as a reference regarding the results of the inserts manufactured with ADAM technology. The designation of the commercial inserts is DCMT 11T308–14 IC20 (ISO 13,399–1:2006), fabricated by ISCAR (ISCAR Ibérica, S.A., Cerdanyola, Barcelona, Spain) and with a Wolfram Carbide (WC—Co) hardness of 90–92 HRA. These are uncoated 55° rhombic positive inserts, recommended for semi-finishing and finishing turning operations, showing a good chip control with medium feed rates [68] (Fig. 1).

The material employed in the fabrication of the Additive Manufacturing inserts was Markforged H13 tool steel (Waltham, Massachusetts, USA). H13 steel is a suitable material for hot work tools, offering a good compromise between hardness and fracture toughness at high temperatures, as well as good resistance to abrasive wear. Specifically, the H13 tool steel is supplied as bound-powder filament to facilitate melting and deposition. H13 steel is designed to withstand high temperature or shear conditions. The balanced alloy content and hardness characteristic of these steels results in minimal distortion during hardening and facilitates cooling. Among tool steels, it presents an excellent combination of high toughness and fatigue resistance, making it particularly suitable for wear-resistant and high-temperature applications, essential conditions in a cutting tool. The chemical composition of H13 tool steel (Markforged) and its principal mechanical characteristics are shown in Table 3.

H13 tool steel records an elastic modulus of 215 GPa at 20 °C. with about 800 MPa of yield strength (0.2 %) and 1200 MPa of Breaking Strength (ASTM E8). H13 steel has an average hardness value of 40 HRC, once sintered (according to the manufacturer). In this work, a sintering and subsequent annealing process was carried out in order to reduce brittleness during machining; this produced a decrease in hardness up to average values of 31 HRC. The Rockwell D hardness scale showed an average value of 22.17 compared to 55.64 HRD for sintering without annealing. Rockwell B test presented a slight difference between the two processes (116 HRB for sintering and 106 HRB for sintering and annealing) [69].

### 2.3. Additive manufacturing of cutting inserts

Once the geometrical characteristics of the commercial insert were identified, the insert was manufactured by the selected Additive Manufacturing process, simplifying the chipbreaker (Fig. 2) and applying the main manufacturing parameters listed in Table 4.

The equipment used in this work was the Markforged Metal X System, with Atomic Diffusion Additive Manufacturing (ADAM) technology. It consists of a process in which three different devices take part: the first, the printing equipment, forms the parts by depositing a molten filament composed of metal powder and binder material, obtaining the so-called "green parts". In next step, the green part is subjected to a washing process (Debbinding in Wash-1) in which most of the binder material is eliminated in a chemical process. After washing, a sintering process is carried out on the part in a controlled atmosphere furnace (Sinter-1). Here, the rest of the binder is eliminated in a thermal operation and the part is completely sintered, resulting in final parts that are largely isotropic in structure. The advantages of this technology are its relatively low cost, its high safety in the workplace and its versatility for different applications.

Currently, Additive Manufacturing has an essential characteristic, the deposition of material layer by layer in a horizontal plane. Therefore, parts manufactured with this technology present a strong anisotropy with respect to the direction perpendicular to the deposition plane. Considering that condition, the position of the parts was determined in order to ensure that their layers presented the greatest resistance to the load to which they would be subjected in the machining process, with an orientation of the inserts in a horizontal plane and showing the filament deposition pattern on the upper surface of the cutting inserts (Fig. 3).

### 2.4. Turning equipment

Turning operations were performed on a Pinacho S-90/180 lathe (Metalúrgica Torrent S.A., Castejón del Puente, Huesca, Spain). Reference tests were established using the commercial inserts (ISCAR, DCMT11T308–14 IC20) to compare them with those from the AM inserts, using the same working conditions and parameters. Machining operations were carried out under different lubrication conditions, both

**Table 3**
H13 Tool steel composition provided by the supplier.

| | Cr | Mo | Si | V | C | Mn | P | S | Fe |
|---|---|---|---|---|---|---|---|---|---|
| % | 4.7–5.5 | 1.3–1.7 | 0.8–1.2 | 0.8–1.2 | 0.3–0.45 | 0.2–0.5 | Max. 0.03 | Max. 0.03 | rest |

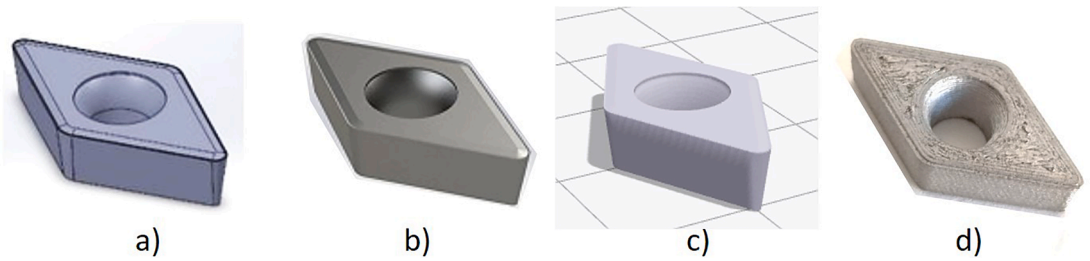


**Fig. 2.** a), b), c) Simulation of the insert printing in virtual environment d) real insert by AM.

**Table 4**
Main manufacturing parameters.

| Layer height (mm) | Nozzle diameter (mm) | Infill (%) | Metal Volume ($cm^3$) | Print time (min) | Wash time (h) | Dry time (h) | Sinter time |
|---|---|---|---|---|---|---|---|
| 0.125 | 0.4 | Solid | 0.52 | 84 | 12 | 4 | 1d 15 h 16 min |

dry and lubricated with the cutting emulsion *Taladrina Blanca Plus* (Quimicrem, Alaquás, Valencia, Spain), suitable for steel and aluminium machining.

### 2.5. Roughness measurements

For the study of the surface finish, 5 longitudinal sections (T1-T5) were considered on each of the machined specimens, along 4 generatrixes arranged at 90° intervals (G1-G4) between each of them. The beginning of the first section starts 30 mm from the area of first contact with the cutting edge and each successive section consists of 30 mm (Fig. 4). The roughness parameter *Ra* (roughness average) and *Rz* (maximum height) were analysed using the Mitutoyo SJ-210 roughness tester (Mitutoyo España, Elgoibar, Guipúzcoa, Spain), with a sampling length of 0.8 mm, an evaluation length of 4 mm and a total length (evaluation length plus start and finish lengths) of 4.8 mm

The configuration of the measurement conditions with the selected equipment and the specification of the evaluation parameters were carried out in accordance with the requirements of ISO 4287 [70], UNE-EN ISO 1302 [71].

### 2.6. Temperature monitoring during the turning process

Regarding the thermographic study, the temperatures reached in the machining processes came from the energy dissipated in the cutting process. Extreme temperature in the cutting zone reduces the mechanical strength, rigidity, hardness, and wear resistance of the tool and, consequently, the macro and microgeometric characteristics of the parts were affected. The thermographic analysis was performed with an Optris PI640i camera, with a range of −20 °C to 900 °C, being considered two study zones: the cutting zone, which corresponds to the fixed area along which the tool runs in the machining process and the hot zone that moves continuously in search of the highest temperature point in the camera's field of view (Fig. 5). The following situations can be possible:

a) Hot Area Temperature > Cutting Area Temperature. At this point the hot area is outside the cutting area (chip, workpiece, etc.) and moves to another hot spot.
b) Cutting Area Temperature ≥ Hot Area Temperature. The point of highest temperature is inside the Cutting Area.

In the test example (II-1) in Fig. 5 it can be seen that initially there is an alternation of hot spot values between the shear zone and the hot zone outside the shear zone. This is due to the fact that at the beginning the distribution of the hot spots is essentially uniform. From the first minute of the machining test, the cutting zone is the one containing the highest temperature points.

### 2.7. Design of experiments (DoE)

The methodology employed in this study consisted of two phases. The first phase involved an initial approach to the behaviour of the chosen material (H13 tool steel) which was subjected to an annealing treatment in order to reduce possible residual stresses generated during the sintering process. In the second phase, design parameters were refined, studying their behaviour by analysing the roughness generated on the specimens and evaluating the temperature evolution in the areas affected by the machining. Additionally, a qualitative study was conducted on the insert wear and the type of chip generated.

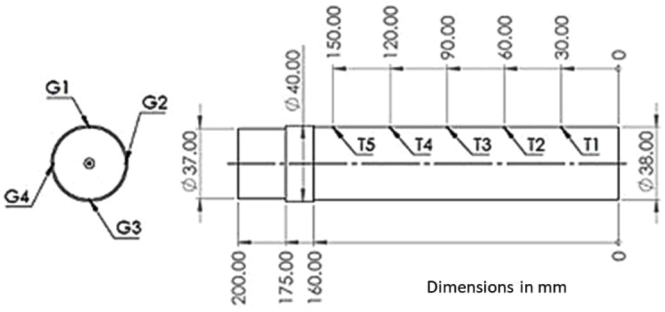


**Fig. 4.** Specimen geometry, sections and generatrixes.

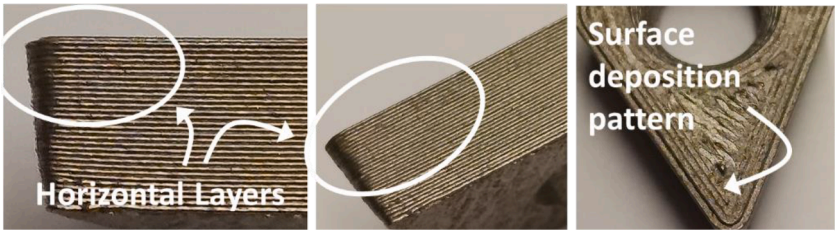


**Fig. 3.** Material layers detail.

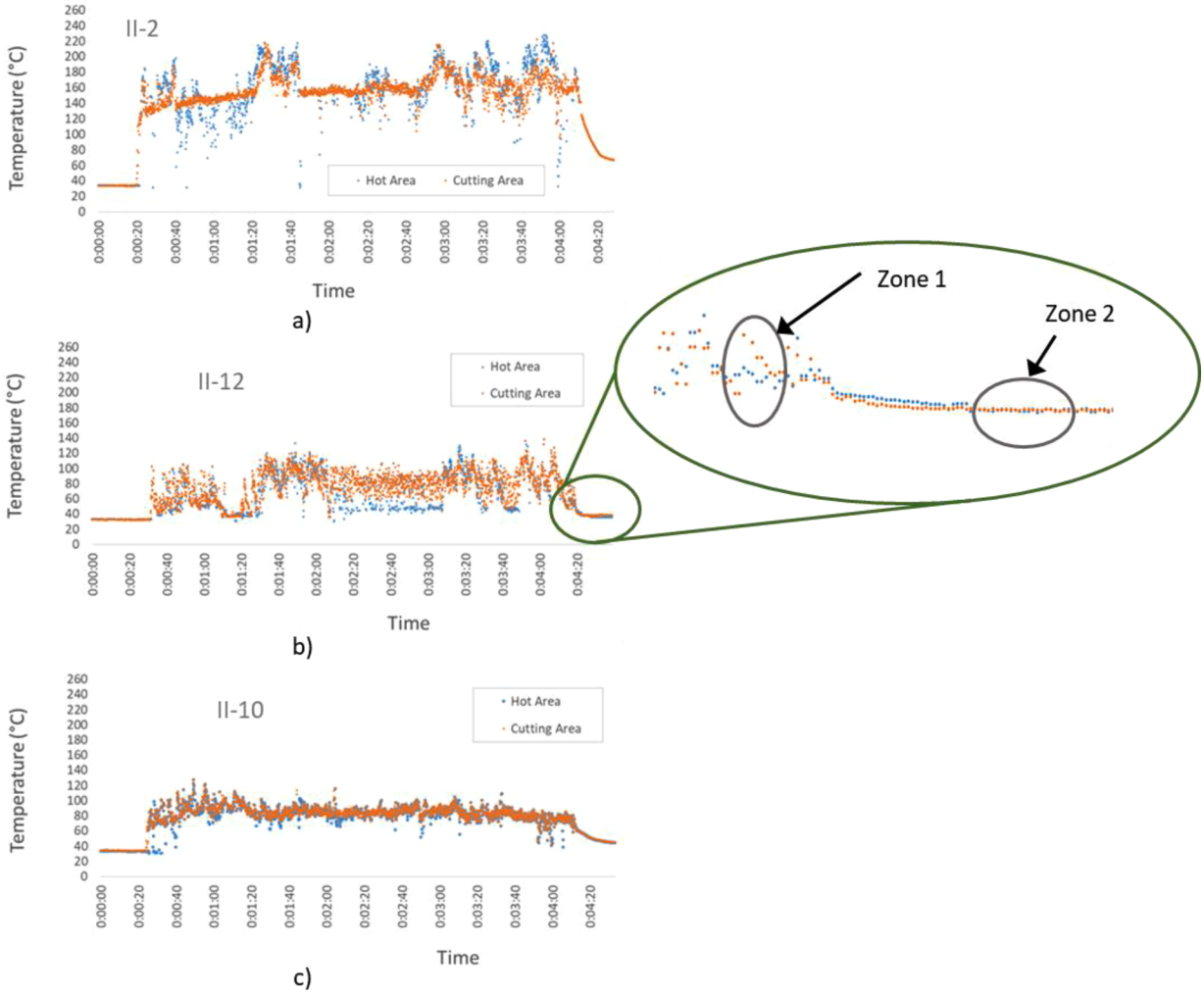


**Fig. 5.** Hot areas (blue) and cutting areas (orange) with $Vc_2$ and $f_1$. a) II-2 b) II-12 c) II-10.

**Table 5**
Testing values on phase I: cutting speed, feed rate, depth of cut, test length and lubrication.

| N° Test with AM H13 insert | N° Test with commercial insert | Cutting speed $V_c$ (m/min) | Feed rate f (mm/r) | Depth of cut $a_p$ (mm) | Test length L (mm) | Lubrication |
|---|---|---|---|---|---|---|
| A-1 | B-1 | 40 | 0.1 | 1 | 40 | No |
| A-2 | B-2 | 60 | | | | |
| A-3 | B-3 | 80 | | | | |
| A-4 | B-4 | 100 | | | | |
| C-1 | | 40 | | 1.5 | 70 | |
| C-2 | | 100 | | | | |
| D-1 | | 20 | | 1 | 80 | Yes |
| D-2 | | 40 | | | | |

In relation to the first phase (phase I), and given the lack of knowledge of the mechanical behaviour that the AM inserts could present, the inserts were tested in two stages, a first stage (samples A and B) to delimit the range of cutting parameter values to be used, and a second stage (samples C and D), in order to define the parameters of the final study (Table 6). In this second stage (phase I), four cylindrical specimens of 200 mm length and 40 mm diameter are produced. They are subjected to cutting speeds ($V_c$) ranging from 40 to 100 m/min, feed rate ($f$) of 0.1 mm/r and depths of cut ($a_p$) of 1 and 1.50 mm. The machining length of

**Table 6**
Testing values on phase II: cutting speed, feed rate, depth of cut and lubrication.

| N° Test with AM H13 insert | N° Test with commercial insert | Cutting speed $V_c$ (m/min) | Feed rate f (mm/r) | Depth of cut $a_p$ (mm) | Lubrication |
|---|---|---|---|---|---|
| II-1 | | 40 | 0.1 | 1 | No |
| II-2 | | | | | |
| II-3 | | | | | |
| II-4 | | | | | |
| | II-5 | | | | No |
| II-6 | | 60 | | | No |
| II-7 | | | | | |
| II-8 | | | | | |
| II-9 | | | | | |
| | II-10 | | | | No |
| II-11 | | | 0.15 | | Yes |
| II-12 | | 40 | | | |
| II-13 | | | | | |
| II-14 | | | | | |
| | II-15 | | | | No |
| II-16 | | | | | Yes |
| II-17 | | 60 | | | |
| II-18 | | | | | |
| II-19 | | | | | |
| | II-20 | | | | No |

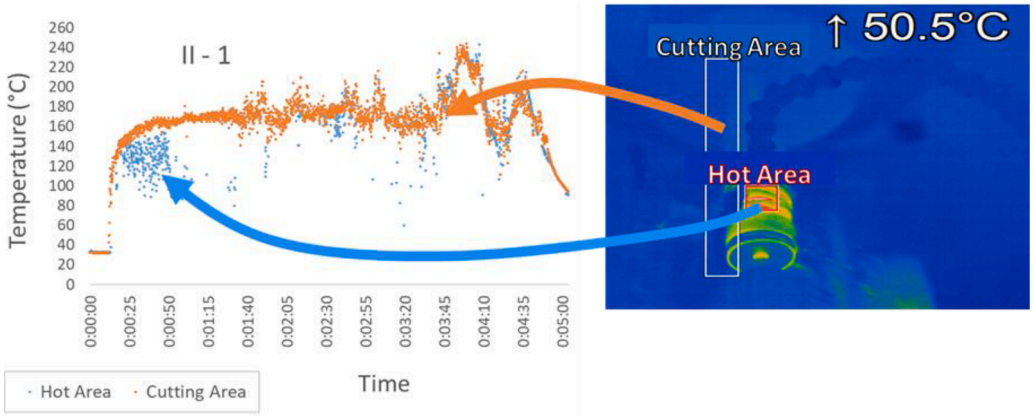


**Fig. 6.** Example of thermographic analysis performed with an Optris PI640i camera.

the specimens was divided into 4 sections, on which the values of the cutting parameters were applied. Results provided the necessary information to establish the behaviour of the commercial and AM inserts, with and without lubrication (Table 5).

Based on this preliminary study, a second more detailed analysis (phase II) was developed by designing a Latin Square. This included four testing combinations with two cutting speeds and two feed rates. From this, both the roughness of the machined specimens and the temperatures generated during the tests were quantitatively studied, as well as the type of chip and the wear of the inserts in all combinations.

Due to the irregularity in the surface finish observed in the specimens of the preliminary study, especially for high values of cutting speed ($Vc$), a new range of $Vc$ values were defined. On the other hand, the feed rate ($f$) was extended to two options. The Latin Square with the different testing values is displayed in Table 6. The depth of cut value is kept constant at $a_1$=1 mm in all the experiments included in this phase.

For each combination of this Latin square, two machining operations with AM inserts in dry process, two with AM inserts with lubrication and finally one machining operation with commercial inserts in dry process were carried out. Therefore, the total number of tests was 20. The reason for doing two repetitions with AM inserts is because there is no record of a similar testing and it is necessary to evaluate the repeatability.

## 3. Results and discussion

### 3.1. Thermal analysis

Tests shown in Fig. 6 (II-2, II-12 and II-10 with $Vc_2$ (60 m/min) and $f_1$ (0.1 mm/r)) provide insight into the temperatures generated in the different areas. In the case of II-2 (AM insert without lubrication), the mean temperature is observed to be approximately 160 °C, with some points reaching up to 200 °C. In II-12 (AM insert with lubrication), the mean temperature was reduced to approximately 80 °C, with a greater dispersion of results due to the irregular nature of the cooling applied. Lastly, II-10 (commercial insert in dry process) provides a similar mean temperature value to II-7, but with a significant reduction in the dispersion of results with respect to it. As illustrated in the same figure, the temperatures of the cutting zone and the hot zone outside it are the same in the test with lubricated AM inserts, even with lower values in the latter zone due to the decrease in its temperature due to the combined effect of the zone not being the machining zone and the cooling effect of the lubrication (Zone 1, Fig. 6). Once machining is completed, the two zones reach the same temperature. (Zone 2, Fig. 6).

From a general perspective, considering the set of tests performed according to the four combinations of $V_c$ ($V_{c1}$ = 40 m/min and $V_{c2}$ = 60 m/min) and $f$ ($f_1$ = 0.1 mm/r and $f_2$ = 0.15 mm/r) defined in, several considerations can be established: in the cutting zones, the tests conducted in dry conditions on AM cutting inserts (II-1, II-2, II-3, II-4, II-6, II-7, II-8, II-9) provided the highest temperature values, with an average value of 155 °C corresponding to the all four combinations of cutting speeds ($V_c$) and feed rates ($f$). In the case of AM cooled cutting inserts (II-11. II-12, II-13, II-14, II-16, II-17, II-18, II-19), the average temperature value dropped to 48 °C, and for tests on Commercial inserts in dry conditions (II-5, II-10, II-15, II-20), temperatures positioned at an intermediate level with an average temperature of 85 °C (Fig. 7).

As is shown in Fig. 7, the variations in $V_c$ and $f$ do not represent any significant change in the temperatures generated in the cutting zone. With commercial inserts, there was a slight increase in temperatures with the increase of both machining parameters, but hardly significant. For the set of tests is observed that the average temperatures remained constant around 98 °C. In a similar study on the hot areas, the evolution of the temperatures in any of the combinations and for each of the tests

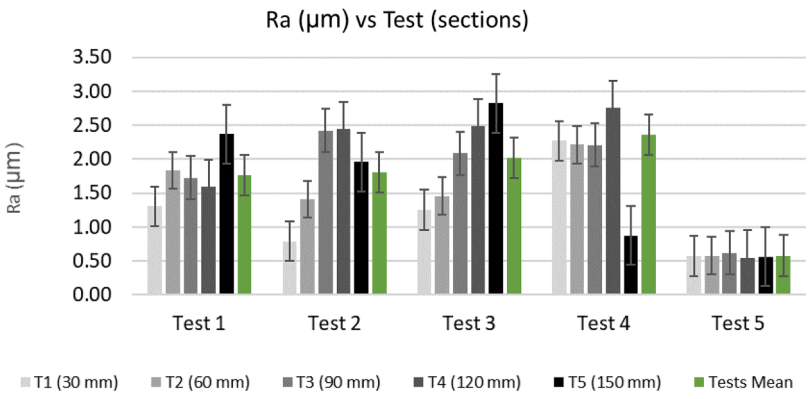


**Fig. 7.** Ra values vs Tests (sections) with Vc1f1 parameters.

**Table 7**
Ra values vs Tests (sections) with $Vc_1f_1$ parameters.

| Ra (μm) | T1 Mean | T2 Mean | T3 Mean | T4 Mean | T5 Mean | Total Mean |
|---|---|---|---|---|---|---|
| **Test 1. AM Dry** | 1.31 ± 0.16 | 1.84 ± 0.36 | 1.72 ± 0.60 | 1.59 ± 0.17 | 2.37 ± 0.04 | 1.76 ± 0.27 |
| **Test 2. AM Dry** | 0.79 ± 0.20 | 1.41 ± 0.49 | 2.42 ± 0.91 | 2.44 ± 0.81 | 1.96 ± 0.83 | 1.80 ± 0.65 |
| **Test 3. AM Lubricated** | 1.25 ± 0.08 | 1.46 ± 0.18 | 2.09 ± 0.21 | 2.48 ± 0.38 | 2.82 ± 0.09 | 2.02 ± 0.19 |
| **Test 4. AM Lubricated** | 2.27 ± 0.31 | 2.21 ± 0.83 | 2.20 ± 0.14 | 2.75 ± 0.70 | 0.87 ± 0.16 | 2.35 ± 0.49 * |
| **Test 5. Commercial** | 0.57 ± 0.09 | 0.58 ± 0.08 | 0.62 ± 0.06 | 0.54 ± 0.08 | 0.56 ± 0.09 | 0.58 ± 0.08 |

were practically coincident, offering average temperatures of 99 °C.

The most decisive influence on the machining process and insert wear comes from the higher temperatures reached in the tests carried out with dry AM inserts (Tests 1 and 2), since this caused the appearance of a built-up edge (Fig. 12). Particularly, this phenomenon appeared in the combinations with higher feed rates (f2).

### 3.2. Roughness analysis

Table 7 and Fig. 8 show the mean values of the roughness parameters *Ra* and Fig. 9 and Table 8 show *Rz* roughness parameters, for $Vc_1f_1$ turning variables, for each of the 5 sections and in each of the tests established. It is observed that the evolution of the results was practically the same for both parameters; commercial inserts (II-5, II-10, II-15, II-20) show very similar values in all the sections of the specimens, which indicates that the wear generated in the cutting tool remained constant and that the lengths and testing time did not modify their behaviour significantly (mean deviations of *Ra* from 0.54 μm (T4) to 0.62 μm (T3).

The result of section 5 (T5) in Test 4 was excluded from the calculation of the overall average since the insert broke for reasons beyond the control of the test procedure.

According to Figs. 9 and 8, Test 3 (AM insert with lubrication (II-11, II-12, II-13, II-14)), shows an evolution of the surface finish compatible with the increase in insert wear (1.25 μm (T1) to 2.82 μm (T5). However, in Test 4 (II-16, II-17, II-18, II-19) (same conditions as Test 3) the behaviour in section 5 displays a notable reduction in roughness, which could be due to the inadequate effect of the lubrication, which generated a built-up edge (BUE) such that the insert "slides" on the machined surface. Tests 1 and Test 2 (II-1, II-2, II-3, II-4 and II-6, II-7, II-8, II-9) also

**Table 8**
Rz values vs Tests (sections) with Vc1f1 parameters.

| Rz (μm) | T1 Mean | T2 Mean | T3 Mean | T4 Mean | T5 Mean | Total Mean |
|---|---|---|---|---|---|---|
| **Test 1. AM Dry** | 7.59 ± 0.87 | 10.41 ±2.25 | 10.36 ±3.85 | 9.09 ± 0.67 | 13.70 ±0.83 | 10.23 ± 1.69 |
| **Test 2. AM Dry** | 4.49 ± 0.20 | 9.00 ± 3.31 | 13.30 ±4.36 | 13.95 ±3.29 | 11.71 ±3.22 | 10.49 ± 3.02 |
| **Test 3. AM Lubricated** | 7.35 ± 0.39 | 9.14 ± 1.42 | 11.05 ±0.56 | 12.84 ±1.71 | 16.49 ±0.66 | 11.37 ±0.95 |
| **Test 4. AM Lubricated** | 12.12 ±1.34 | 12.91 ±2.46 | 11.61 ±1.04 | 13.96 ±3.10 | 5.24 ± 0.45 | 11.17 ±1.68 * |
| **Test 5. Commercial** | 3.13 ± 0.37 | 3.25 ± 0.44 | 3.55 ± 0.59 | 3.29 ± 0.36 | 3.43 ± 0.23 | 3.33 ± 0.40 |

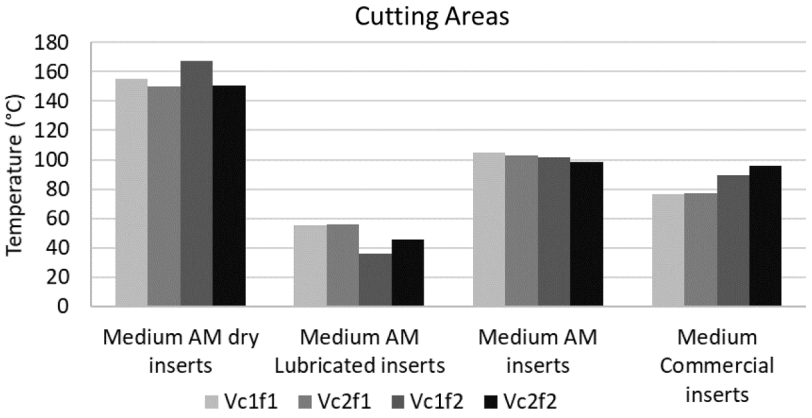


**Fig. 8.** Average temperature in cutting areas.

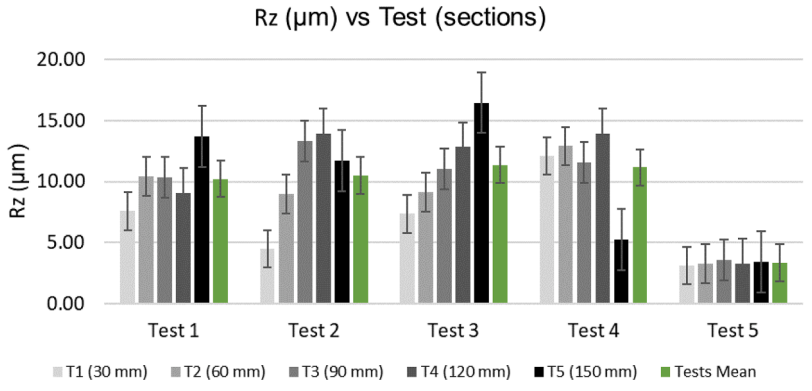


**Fig. 9.** Ra values vs Tests (sections) with Vc1f1 parameters.

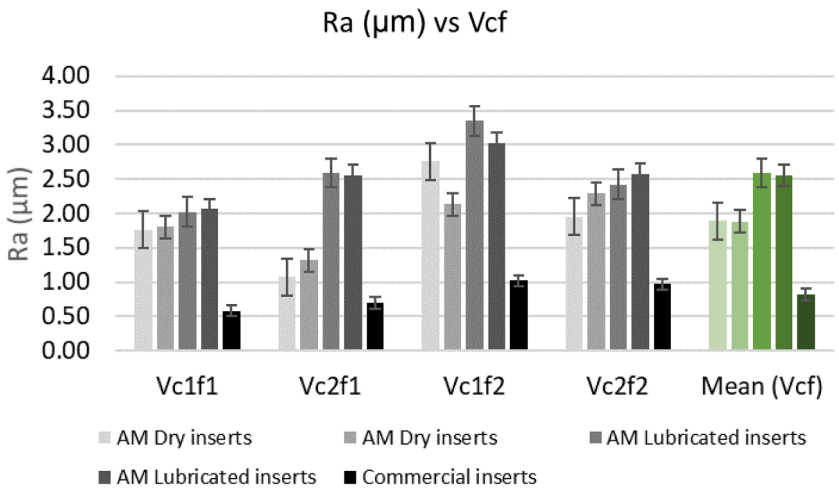


**Fig. 10.** Ra vs Vcf combinations and tests.

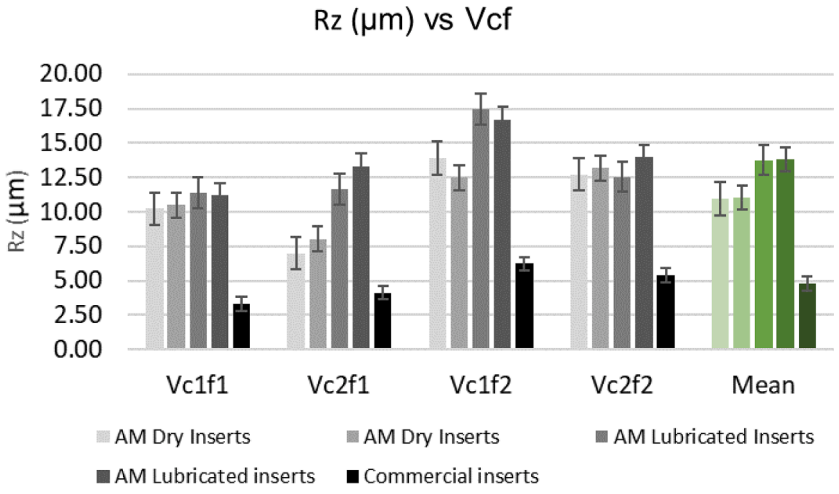


**Fig. 11.** Rz vs Vcf combinations and tests.

present similar behaviour, typical of the irregular character of the BUE formation, with minimum and maximum Ra values of 1.31 μm (T1) to 2.37 μm (T5) and 0.79 μm (T1) to 2.44 μm (T4) respectively. As previously stated, test with commercial inserts T5 (II-5, II-10, II-15, II-20) exhibits the more stable behaviour, with the lowest roughness values.

On the other hand, Figs. 10 and 11 detail the evolution of the roughness values (*Ra* and *Rz,* respectively) for each combination of *Vc* and *f* parameters considered in the design of experiment. In terms of a natural evolution of tool wear and, therefore, lower roughness, the most favourable parameter combinations are Vc1f1 and Vc2f2, with Vc1f1 providing the lowest roughness values in all the tests carried out. The third combination ($Vc_1f_2$) presents a higher mean value for the set of tests, which implies the decisive influence of the feed rate ($f_2 = 0.15$ mm). Increasing the cutting speed (Vc) gives an increase in roughness in the tests with lubricated inserts (Tests 3 and 4) and a reduction in the case of dry machining (Tests 1 and 2) when the feed rate is maintained at its lowest value (f1). This influence is not so evident when the feed rate takes its highest value (f2). The mean values of the four combinations (green columns) show the roughness values which are similar for the same test conditions (Tests 1 and Test with AM inserts in dry conditions,

**Table 9**
Ra vs Vcf combinations and tests.

| | Ra (μm) | | | | | | | |
|---|---|---|---|---|---|---|---|---|
| | $Vc_1f_1$ Mean | $Vc_2f_1$ Mean | $Vc_1f_2$ Mean | $Vc_2f_2$ Mean | $Vc_{1-2}f_1$ Mean | $Vc_{1-2}f_2$ Mean | $Vc_1f_{1-2}$ Mean | $Vc_2f_{1-2}$ Mean |
| **Test 1. AM Dry** | 1.76 | **1.07** | *2.77* | 1.95 | **1.42** | *2.36* | 2.27 | 1.51 |
| **Test 2. AM Dry** | 1.80 | **1.32** | 2.13 | *2.29* | **1.56** | *2.21* | 1.97 | 1.81 |
| **Test 3. AM Lubricated** | **2.02** | 2.59 | *3.35* | 2.42 | **2.31** | *2.89* | 2.69 | 2.51 |
| **Test 4. AM Lubricated** | **2.35** | 2.56 | *3.03* | 2.58 | **2.46** | *2.81* | 2.69 | 2.57 |
| **Test 5. Commercial** | **0.58** | 0.70 | *1.02* | 0.97 | **0.64** | *1.00* | 0.80 | 0.84 |
| **Tests AM Dry (1,2)** | 1.78 | **1.20** | 2.45 | 2.12 | **1.49** | *2.29* | 2.12 | 1.66 |
| **Tests AM Lubricated (3,4)** | **2.19** | 2.58 | *3.19* | 2.50 | **2.38** | *2.85* | 2.69 | 2.54 |
| **Tests AM (1,2,3,4)** | **1.98** | **1.89** | *2.82* | 2.31 | **1.93** | *2.57* | 2.40 | 2.10 |

| | $a_p = 1\ mm$ | | | |
|---|---|---|---|---|
| | $Vc_1f_1$ | $Vc_2f_1$ | $Vc_1f_2$ | $Vc_2f_2$ |
| AM Dry inserts | II-1 Ra =1.76 (μm) Ra(T5) =2.37 (μm) Rz =10.23 (μm) | II-2 Ra =1.07 (μm) Ra(T5) =1.36 (μm) Rz =6.98 (μm) | II-3 Ra =2.76 (μm) Ra (T5) =5.03 (μm) Rz =13.91 (μm) | II-4 Ra =1.95 (μm) Ra(T5) =2.41 (μm) Rz =12.71 (μm) |
| |  |  |  |  |
| | Moderate BUE | Moderate BUE | Plastic def. of the tip | Plastic def. of the tip |
| AM Dry inserts | II-6 Ra =1.80 (μm) Ra(T5) =1.96 (μm) Rz =10.49 (μm) | II-7 Ra =1.32 (μm) Ra(T5) =1.85 (μm) Rz =8.02 (μm) | II-8 Ra =2.13 (μm) Ra(T5) =1.85 (μm) Rz =12.47 (μm) | II-9 Ra =2.29 (μm) Ra(T5) =1.96 (μm) Rz=13.18 (μm) |
| |  |  |  |  |
| | Moderate BUE | Moderate BUE | High BUE | High BUE |
| AM Lubricated inserts | II-11 Ra =2.02(μm) Ra(T5) =2.82 (μm) Rz =11.37 (μm) | II-12 Ra =2.59 (μm) Ra(T5) =2.86 (μm) Rz =11.64 (μm) | II-13 Ra =3.35 (μm) Ra(T5) = ---- (μm) Rz =17.46 (μm) | II-14 Ra =2.42 (μm) Ra(T5) =2.64 (μm) Rz =12.55 (μm) |
| |  |  | 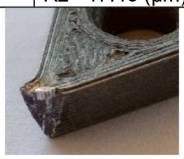 | 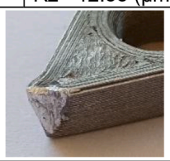 |
| | Low BUE + Plastic def. of the tip | Low BUE + Plastic def. of the tip | Plastic def. of the tip | Plastic def. of the tip |
| AM Lubricated inserts | II-16 Ra =2.06 (μm) Ra(T5) =0.87 (μm) Rz =11.17 (μm) | II-17 Ra =2.56 (μm) Ra(T5) =3.45 (μm) Rz =13.33 (μm) | II-18 Ra =3.03(μm) Ra(T5) =1.17(μm) Rz =16.71 (μm) | II-19 Ra =2.58 (μm) Ra(T5) =2.63(μm) Rz =13.98 (μm) |
| | 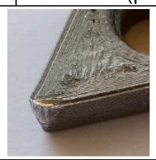 |  | 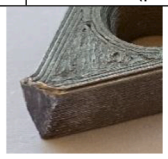 |  |
| | Plastic def. of the tip | Low BUE | Plastic def. of the tip | Low BUE + Plastic def. of the tip |
| Commercial inserts | II-5 Ra =0.58 (μm) Ra(T5) =0.56 (μm) Rz =3.33 (μm) | II-10 Ra =0.70 (μm) Ra(T5) =0.75 (μm) Rz =4,12 (μm) | II-15 Ra =1.02 (μm) Ra(T5) =0.72 (μm) Rz =6.22 (μm) | II-20 Ra =0.97 (μm) Ra(T5) =1.02 (μm) Rz =5.39 (μm) |
| | 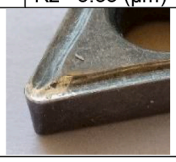 | 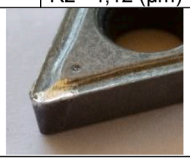 | | |
| | Mínimum wear | Mínimum wear | Mínimum wear | No damage |

**Fig. 12.** Cutting inserts wear.

Tests 3 and 4 with AM inserts and lubrication and Test 5 with commercial inserts). Rz results follow the same trend.

Results also show the low influence of the cutting speed ($Vc_1 = 40$ m/min, $Vc_2 = 60$ m/min) on the roughness. As is seen in Table 9, the lowest values of Ra are found in columns $Vc_1f_1$ and $Vc_2f_1$ (in bold). This suggests that the decisive parameter for this reduced roughness is the feed rate $f_1$ ($f_1 = 0.10$ mm/r). Similarly, the highest roughness values (in italics) are shown in columns $Vc_1f_2$ and $Vc_2f_2$, corresponding to the highest feed rate ($f_2 = 0.15$ mm/r). The arithmetic mean of these pairs of columns is reflected in the last four columns of Table 9 observing that the lowest values of these means appear in $Vc_{1-2}f_1$ (bold) and the highest in $Vc_{1-2}$ $f_2$ (italics).

The mean increase in Ra when modifying the feed rate value is around 35 % for tests with dry AM inserts. This figure is 16 % when the AM inserts are lubricated during the test and reaches 25 % for all AM inserts that were tested. For the commercial inserts, this increase is close to 36 %, which is very similar to that observed for the dry AM inserts.

The last three rows of Table 9 show the averages roughness values for

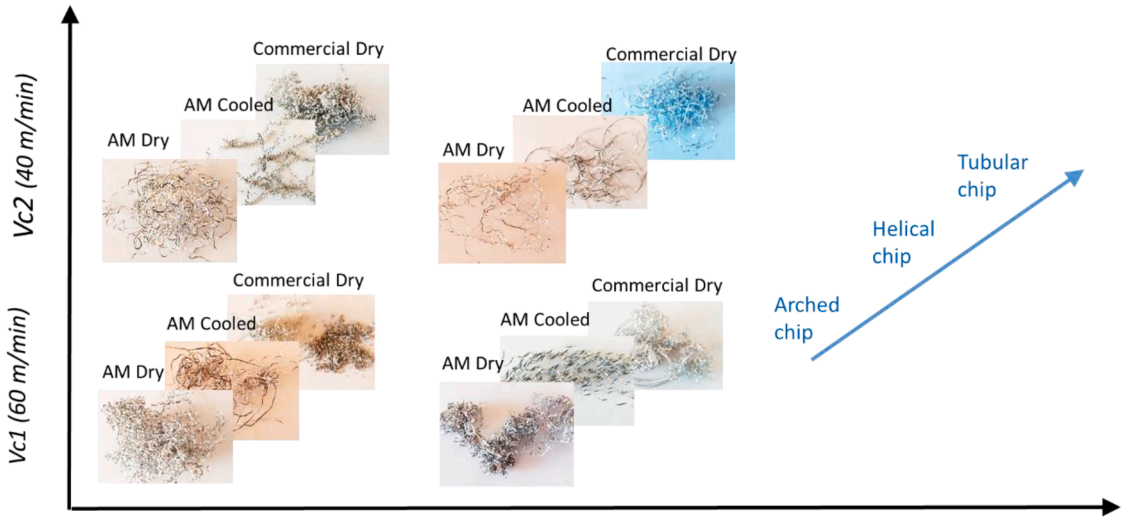


**Fig. 13.** Chip morphology.

the tests involving dry AM inserts (Tests 1 and 2), those with lubricated AM inserts (Tests 3 and 4) and all the tests carried out with AM inserts (Tests 1, 2, 3 and 4). From these results, it was possible to deduce the optimal combination of parameters regarding the roughness characteristic, both for the commercial inserts and the AM inserts that were the subject of the study.

In particular, the combination of parameters $Vc_2f_1$ ($Vc_2 = 60$ m/min, $f_1 = 0.1$ mm/r) is the most effective in terms of achieving the lowest

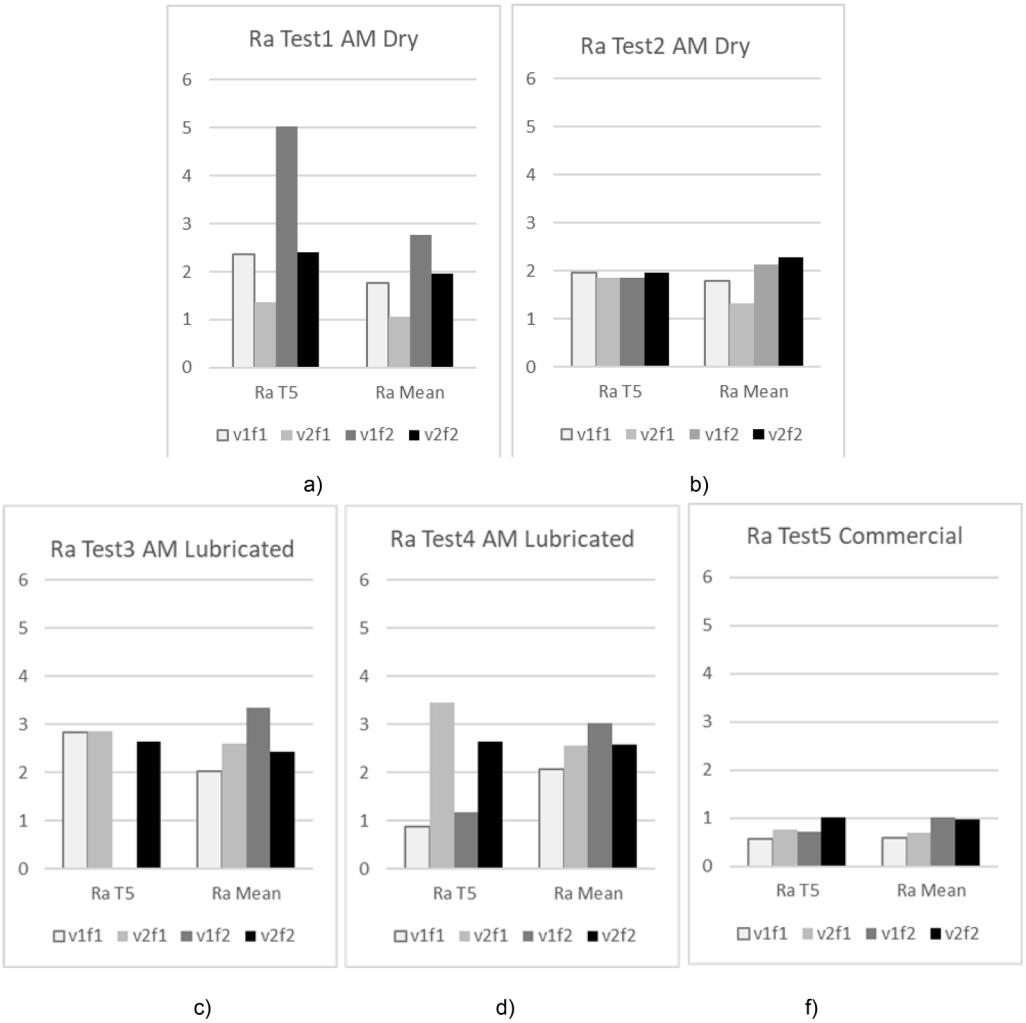


**Fig. 14.** Ra Mean vs Ra T5: a) Test 1 b) Test 2 c) Test 3 d) Test 4 e) Test 5.

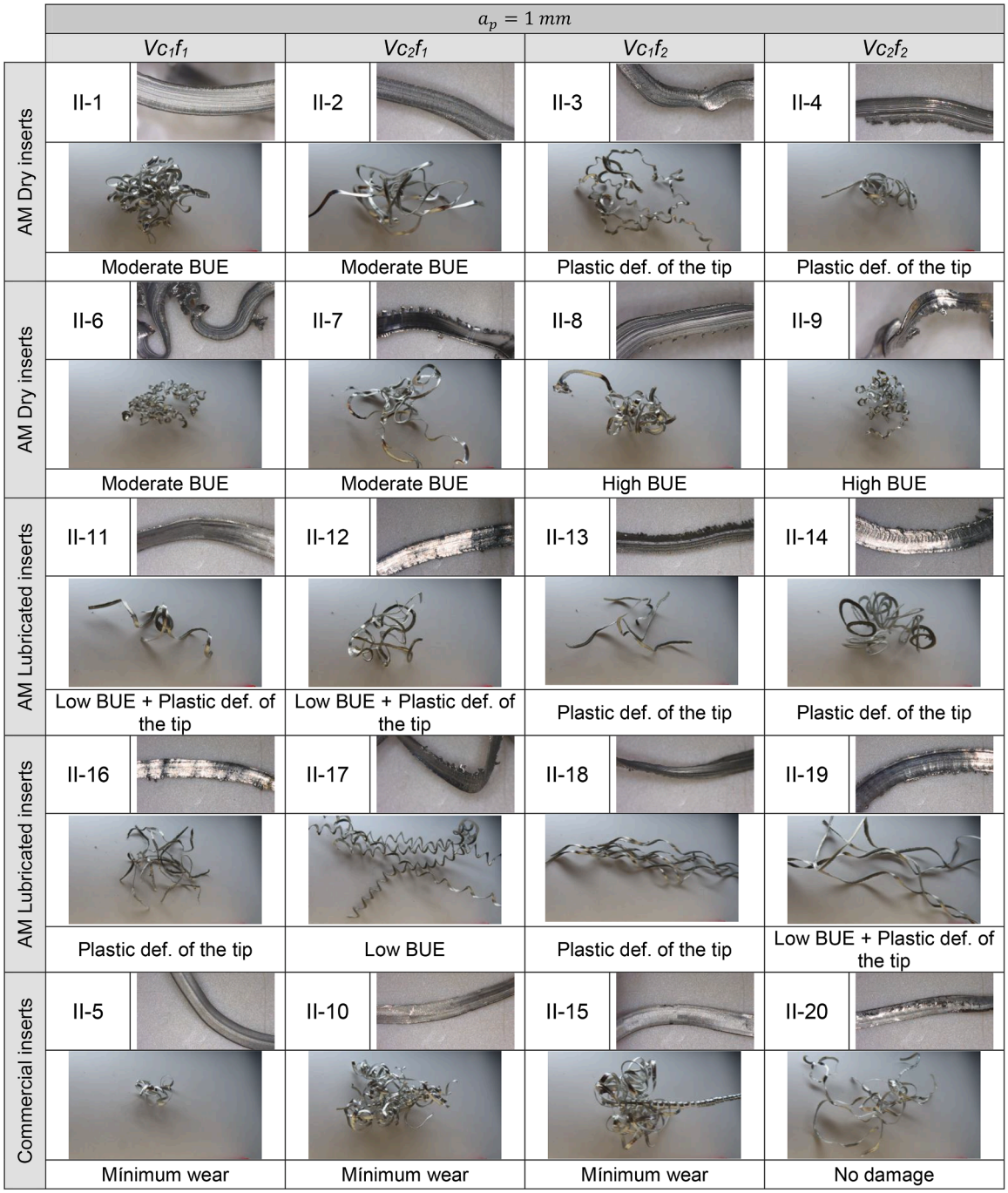


**Fig. 15.** Chip morphology II.

average Ra values in dry AM insert. Consequently, this combination of parameters is the recommended option in the present study. With regard to commercial inserts and AM inserts with lubrication (which may be relevant in other contexts), the optimal parameter combination is $Vc_1f_1$ ($Vc_1 = 40$ m/min, $f_1 = 0.1$ mm/r).

### 3.3. Analysis of the cutting edge condition and insert wear

Insert wear has been analysed through visual inspection since this study proposes a possible viability of manufacturing cutting inserts with Additive Manufacturing as an alternative to traditional manufacturing processes such as powder metallurgy.

In general, the annealing process applied to the inserts manufactured by AM in order to reduce the brittleness of the cutting edge resulted in an increased occurrence of built-up edge (BUE) and even, in some cases, plastic deformation of the tip. As shown in Fig. 12, there is no BUE on the commercial inserts (Test 5) and wear is minimal. Even under $Vc_2$ and $f_2$ conditions there is no damage to the cutting edge of the inserts. For the unlubricated AM inserts (Tests 1 and 2), the images show the presence of moderate built-up edges (BUE), which are slightly more pronounced and even with plastic deformation of the tip at cutting speeds of 60 m/min ($Vc_2$). For lubricated AM inserts (Tests 3 and 4), the built-up edge observed was minimal and in those situations where tip deformation occurred, this was lower than that generated under dry conditions. However, the combination of both effects increased the Ra values. The cutting edges in general presented better conditions in lubricated tests

In addition, it can be noticed how in the tests where $f_2$ feed rate is applied (II-3, II-4, II-8, II-9, II-13, II-14, II-18 and II-19) and in some

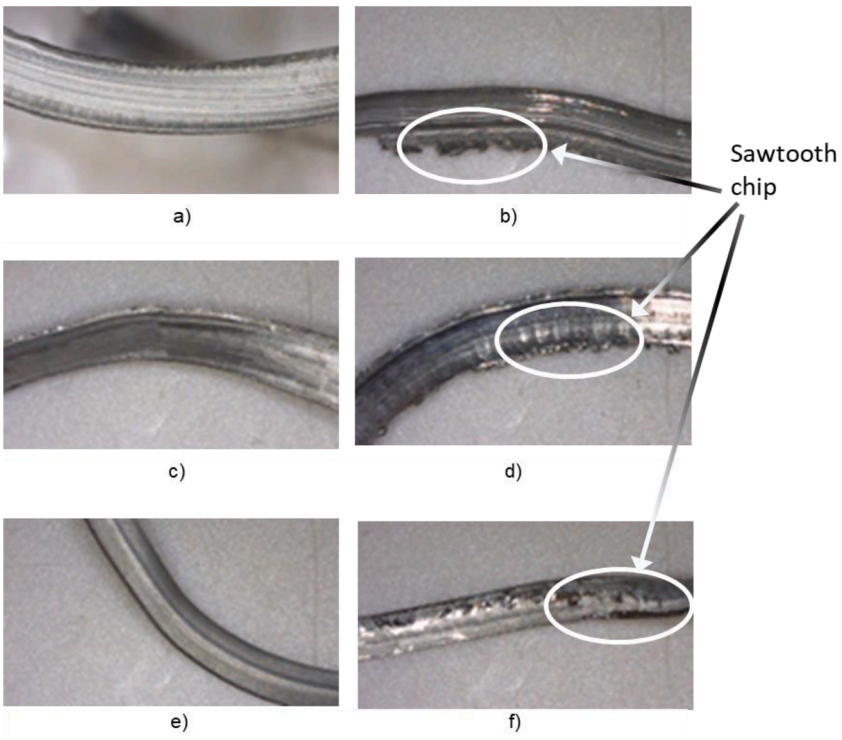


**Fig. 16.** Chip morphology a) AM Dry inserts $Vc_1f_1$ b) AM Dry inserts $Vc_2f_2$ c) AM Lubricated inserts $Vc_1f_1$ d) AM Lubricated inserts $Vc_2f_2$ e) Commercial inserts $Vc_1f_1$ f) Commercial inserts $Vc_2f_2$.

others, such as II-12 and II-17 with $f_1$ and $Vc_2$, the wear of the inserts is significantly higher, corresponding directly to a higher Ra in the specimens.

Fig. 12 shows images of the final state of the tip of the inserts subjected to the different tests. Beside each image, the average Ra value of all the tests and the average Ra value of the last section (T5) are presented (this last value gives a more suitable indication of the final state of the insert). According to this figure, in the cases where BUE is high (tests II-8 and II-9), it is observed that the Ra value (T5) is slightly lower than the average Ra value of the complete test, which is due to the cyclic and unstable behaviour of the BUE. Fig. 13 draws a comparison between the mean Ra values of the different tests and the mean Ra values of the last section (T5) of the tests.

### 3.4. Analysis of chip morphology

With regard to the morphology and appearance of the chips (Fig. 14), dry tests on AM inserts generally produced very long chips with connected arched geometry or tending to be flat, which could be due to the combination of two factors: on the one hand, the absence of chip-breakers in this type of insert limited the formation of tubular chips; on the other hand, the presence of built-up edge, although moderate, determined the different orientation of the chip because of its irregular behaviour. In the tests with cooled AM inserts, the plastic deformation generated at the tip of the tool and the absence of chip breakers resulted in the generation of multiple chip shapes (short flat, tangled or long, curved, helical, etc.). In tests with commercial inserts, the use of chip-breakers and the absence of edge build-up or plastic deformation produced chips with an essentially tubular morphology under all test conditions, with no significant influence of the machining parameters considered since the range of working speeds was within the range defined by the manufacturer (Fig. 15).

Finally, from Fig. 16 it is deduced that the chips which were subjected to the most aggressive conditions and deformation were those from the combination of parameters with the highest values ($Vc_2 = 60$ m/min, $f_2 = 0.15$ mm/r) (Fig. 16b) and d)), especially due to the effect of the higher feed rate $f_2$, even with commercial inserts (Fig. 16f)).

## 4. Conclusions

From this study, based on the results obtained from the tests conducted on EN AW2030 aluminium using commercial cutting inserts and inserts manufactured by Additive Manufacturing, the following conclusions were drawn:

The thermal analysis showed that the average temperature in the cutting zone during the machining process using AM cutting inserts without lubrication was around 155 °C whereas it was about 85 °C for commercial inserts. With lubrication this temperature decreased to around 50 °C. The 70 °C increase between the dry machining processes for both types of cutting inserts is not a significant factor that severely affects the capacity of the new AM inserts. The elevated temperature during the dry machining of AM inserts favoured the formation of BUE on the cutting edge of the insert, which subsequently resulted in an increase rate of insert wear.

With regard to the surface finish, the average roughness (Ra) generated in the three testing groups provided a global average value for dry AM cutting inserts of 1.89 μm, 2.61 μm for AM inserts with lubrication and 0.82 μm with commercial inserts in dry conditions. These values correspond to the mean obtained for the four combinations of established parameters (cutting and feed speeds). Although the difference the results between AM inserts and commercial inserts represent a significant relative increase of those, in absolute terms these values are within an acceptable range for this type of machining process. The maximum roughness parameter (*Rz*) showed the same trend. For the AM inserts, according to the tests carried out on the four different combinations of cutting speed (Vc) and feed rate (f), it was inferred that feed rate was the most influential parameter. Indeed, by modifying the cutting speed and comparing the Ra values for the combinations $Vc_1f_1$ ($Ra = 1.98$ μm) with $Vc_2f_1$ ($Ra = 1.89$ μm) and $Vc_1f_2$ ($Ra = 2.82$ μm) with $Vc_2f_2$ ($Ra = 2.31$ μm) variations of 5 % and 18 % respectively were

obtained. However, when the feed rate was modified and the same comparisons were made: $Vc_1f_1$ ($Ra = 1.98$ μm) with $Vc_1f_2$ ($Ra = 2.82$ μm) and $Vc_2f_1$ ($Ra = 1.89$ μm) with $Vc_2f_2$ ($Ra = 2.31$ μm) the variations achieved by increasing the feed rate were 42 % and 22 % respectively. This influence was reflected in both AM and commercial inserts (in these last, increases of Ra of 13 % for Vc and of 57 % when f is modified). The combination $\mathbf{Vc_2f_1}$ ($Vc_2 = 60$ m/min, $f_1 = 0.1$ mm/r) reached the lowest average values of Ra and was the one that most closely approximated the behaviour of the AM inserts with the commercial ones, both in dry conditions. It can therefore be stated that this combination offers the optimal range for dry AM inserts. For AM inserts with lubricated tests, the most favourable combination deduced was $\mathbf{Vc_1f_1}$ ($Vc_1 = 40$ m/min, $f_1 = 0.1$ mm/r).

Regarding insert wear, AM inserts showed two slightly different evolutions. In testing with lubricated AM tools, minimal built-up edge (BUE) appeared as well as a reduced plastic deformation at the tool tip. This was because the very low cutting temperatures (50 °C) avoided strong adhesion of the aluminium from the specimens to the inserts. In the case of dry AM tools, the highest average machining temperature (155 °C) facilitated the appearance of BUE, and in cases with $Vc_2$=60m/min, the plastic deformation suffered by the cutting edge was much more pronounced. Commercial inserts showed no relevant damage, resulting in the chip shape being essentially tubular. The absence of chipbreaker in the AM inserts (due to design limitations) and the appearance of BUE with its characteristic unstable behaviour, led to the formation of different chip types, such as flat or arched with no signs of breakage, resulting in entangled and elongated chips.

In conclusion, as a result of the study conducted, it can be established that machining cutting inserts produced by additive manufacturing processes present suitable behaviour in service, making it possible to consider them a great alternative to those produced by conventional manufacturing processes.

## Funding

This research did not receive any specific grant from funding agencies in the public, commercial, or not-for-profit sectors.

## Compliance with ethics guidelines

The authors declare that they have no conflict of interest or financial conflicts to disclose.

## CRediT authorship contribution statement

**Francisco Martín-Fernández:** Writing – review & editing, Visualization, Validation, Software, Methodology, Investigation, Data curation, Conceptualization. **María Jesús Martín-Sánchez:** Writing – original draft, Visualization, Methodology, Investigation, Formal analysis, Data curation, Conceptualization. **Guillermo Guerrero-Vacas:** Supervision, Methodology, Formal analysis. **Óscar Rodríguez-Alabanda:** Visualization, Supervision, Methodology.

## Declaration of competing interest

The authors declare that they have no known competing financial interests or personal relationships that could have appeared to influence the work reported in this paper.

## Acknowledgements

The authors want to thank the University of Malaga-Andalucía Tech, International Campus of Excellence.

## Supplementary materials

Supplementary material associated with this article can be found, in the online version, at doi:10.1016/j.rineng.2024.103194.

## Data availability

No data was used for the research described in the article.

## References

[1] I.T. Daniel, B.S. Aondover, T.L. Tyovenda, Prediction of cutting temperature distribution in transient heat conduction of monolayer coated tools based on nonfourier heat conduction during machining of H13 hard steel, Int. J. Eng. Res. Sci. (IJOER) 9 (8) (2023).
[2] K. Rall, D. Loker, C.P. Nikhare, Optimal machine learning for detecting lathe machining parameters, Int. J. Adv. Manufact. Technol. 128 (1–2) (2023), https://doi.org/10.1007/s00170-023-11939-4.
[3] N.S.D. Ab Aziz, N.A. Raof, A.G. Abdul Rahman, A.N. Dahnel, S. Mokhtar, N.K. M. Khairussaleh, Cutting tool performance in turning of AL 7075-t651 aluminium alloy, IIUM Eng. J. 21 (2) (2020), https://doi.org/10.31436/iiumej.v21i2.1227.
[4] M. Nizar, N. Arimatsu, H. Kawamitsu, K. Takai, M. Fukumoto, Study on optimal surface property of WC-Co cutting tool for aluminium alloy cutting, in: IOP Conference Series: Materials Science and Engineering, 2016, https://doi.org/10.1088/1757-899X/114/1/012024.
[5] Z. Siemiatkowski, et al., Study in durability of CR2O3-based ceramic cutting tools, Eng. Rur. Develop. (2023), https://doi.org/10.22616/ERDev.2023.22.TF054.
[6] J. Zhang, J. Wang, G. Zhang, Z. Huo, Z. Huang, L. Wu, A review of diamond synthesis, modification technology, and cutting tool application in ultra-precision machining, Mater. Des. 237 (2024).
[7] S.K. Pattnaik, M. Behera, S. Padhi, P. Dash, S.K. Sarangi, Study of cutting force and tool wear during turning of aluminium with WC, PCD and HFCVD coated MCD tools, Manuf. Rev. (Les. Ulis) 7 (2020), https://doi.org/10.1051/mfreview/2020026.
[8] G. Ramírez, et al., Super-hard DLC coatings as an alternative to polycrystalline diamond for cutting tools: predictive analysis of aluminium alloy surface quality, Lubricants 10 (7) (2022), https://doi.org/10.3390/lubricants10070135.
[9] M.S.A. Bernatskyi, History of technology, Hist. Sci. Technol. 13 (2) (2023).
[10] M.Á. Caminero, A. Romero Gutiérrez, J.M. Chacón, E. García-Plaza, P.J. Núñez, Effects of fused filament fabrication parameters on the manufacturing of 316L stainless-steel components: geometric and mechanical properties, Rapid. Prototyp. J. 28 (10) (2022), https://doi.org/10.1108/RPJ-01-2022-0023.
[11] A. Karolczuk, et al., Heterogeneous effect of aging temperature on the fatigue life of additively manufactured thin-walled 18Ni300 maraging steel tubular specimen, Mater. Des. 237 (2024) 112561, https://doi.org/10.1016/j.matdes.2023.112561.
[12] D. Kong, et al., About Metastable Cellular Structure in Additively Manufactured Austenitic Stainless Steels, 2021, https://doi.org/10.1016/j.addma.2020.101804.
[13] M. Yuan, L. Nyborg, C. Oikonomou, Y. Fan, L. Liu, Y. Cao, Time and temperature dependent softening of a novel maraging steel fabricated by laser metal deposition, Mater. Des. 224 (2022), https://doi.org/10.1016/j.matdes.2022.111393.
[14] S. Banait, C. Liu, M. Campos, M.S. Pham, M.T. Pérez-Prado, Effect of microstructure on the effectiveness of hybridization on additively manufactured Inconel718 lattices, Mater. Des. 236 (2023) 112484, https://doi.org/10.1016/j.matdes.2023.112484.
[15] S.C. Bodner, et al., Inconel-steel multilayers by liquid dispersed metal powder bed fusion: microstructure, residual stress and property gradients, Addit. Manuf. 32 (2020), https://doi.org/10.1016/j.addma.2019.101027.
[16] P. Wood, et al., High strain rate effect on tensile ductility and fracture of AM fabricated Inconel 718 with voided microstructures, Mater. Des. 208 (2021), https://doi.org/10.1016/j.matdes.2021.109908.
[17] M.Q. Shaikh, S. Graziosi, S.V. Atre, Supportless printing of lattice structures by metal fused filament fabrication (MF3) of Ti-6Al-4V: design and analysis, Rapid. Prototyp. J. 27 (7) (2021), https://doi.org/10.1108/RPJ-01-2021-0015.
[18] T.C. Dzogbewu, Laser powder bed fusion of Ti15Mo, Result. Eng. 7 (2020), https://doi.org/10.1016/j.rineng.2020.100155.
[19] A. Arjunan, A. Baroutaji, A. Latif, Acoustic behaviour of 3D printed titanium perforated panels, Result. Eng. 11 (2021), https://doi.org/10.1016/j.rineng.2021.100252.
[20] U. Gürol, S. Dilibal, B. Turgut, H. Baykal, H. Kümek, M. Koçak, Manufacturing and characterizaton of waam-based bimetallic cutting tool, Int. J. 3D Print. Technolog. Digit. Ind. 6 (3) (Dec. 2022) 548–555, https://doi.org/10.46519/ij3dptdi.1210836.
[21] C. Rock, P. Tarafder, L. Ives, T. Horn, Characterization of copper & stainless steel interface produced by electron beam powder bed fusion, Mater. Des. 212 (2021), https://doi.org/10.1016/j.matdes.2021.110278.
[22] T.A. Rodrigues, et al., Steel-copper functionally graded material produced by twin-wire and arc additive manufacturing (T-WAAM, Mater. Des. 213 (2022), https://doi.org/10.1016/j.matdes.2021.110270.
[23] M. Seleznev, J.D. Roy-Mayhew, Bi-metal composite material for plastic injection molding tooling applications via fused filament fabrication process, Addit. Manuf. 48 (2021), https://doi.org/10.1016/j.addma.2021.102375.

[24] B. Wu, et al., Selective crack propagation in steel-nickel component printed by wire arc directed energy deposition, Mater. Des. 237 (2024) 112541, https://doi.org/10.1016/j.matdes.2023.112541.
[25] A. Mussatto, Research progress in multi-material laser-powder bed fusion additive manufacturing: a review of the state-of-the-art techniques for depositing multiple powders with spatial selectivity in a single layer, Result. Eng. 16 (2022), https://doi.org/10.1016/j.rineng.2022.100769.
[26] A. Javed, O. ur R. Shah, S. Ahmad, D. Ahmed, Optimization of viscosity and composition of mixture of Cu powder and acrylate based resin for vat photopolymerization of metal components, Result. Eng. 19 (2023), https://doi.org/10.1016/j.rineng.2023.101307.
[27] T.C. Dzogbewu, N. Amoah, S. Afrifa Jnr, S.K. Fianko, D.J. de Beer, Multi-material additive manufacturing of electronics components: a bibliometric analysis, Result. Eng. 19 (2023), https://doi.org/10.1016/j.rineng.2023.101318.
[28] M.Á. Caminero, A. Romero, J.M. Chacón, P.J. Núñez, E. García-Plaza, G. P. Rodríguez, Additive manufacturing of 316L stainless-steel structures using fused filament fabrication technology: mechanical and geometric properties, Rapid. Prototyp. J. 27 (3) (2021), https://doi.org/10.1108/RPJ-06-2020-0120.
[29] K. Trojan, et al., Microstructure and Mechanical Properties of Laser Additive Manufactured H13 Tool Steel, Metal. (Basel) 12 (2) (2022), https://doi.org/10.3390/met12020243.
[30] M.A. Mahmood, F.G. Alabtah, Y. Al-Hamidi, M. Khraisheh, On the Laser Additive Manufacturing of High-Entropy Alloys: A Critical Assessment of In-Situ Monitoring Techniques and Their Suitability, 2023, https://doi.org/10.1016/j.matdes.2023.111658.
[31] S. Yan, X. He, M. Krüger, Y. Li, Q. Jia, Additive manufacturing of a new non-equiatomic high-entropy alloy with exceptional strength-ductility synergy via in-situ alloying, Mater. Des. 238 (2024).
[32] A.A. Akinwande, O.A. Balogun, A.A. Adediran, O.S. Adesina, V. Romanovski, T. C. Jen, Experimental analysis, statistical modeling, and parametric optimization of quinary-(CoCrFeMnNi)100 –x/TiCx high-entropy-alloy (HEA) manufactured by laser additive manufacturing, Result. Eng. 17 (2023), https://doi.org/10.1016/j.rineng.2022.100802.
[33] A. Baroutaji, A. Arjunan, G. Singh, J. Robinson, Crushing and energy absorption properties of additively manufactured concave thin-walled tubes, Result. Eng. 14 (2022), https://doi.org/10.1016/j.rineng.2022.100424.
[34] Y. Yang, C. Zhang, D. Wang, L. Nie, D. Wellmann, Y. Tian, Additive manufacturing of WC-Co hardmetals: a review, Int. J. Adv. Manufact. Technol. 108 (5–6) (2020), https://doi.org/10.1007/s00170-020-05389-5.
[35] A. Basak, A. Lee, A. Pramanik, K. Neubauer, C. Prakash, S. Shankar, Material extrusion additive manufacturing of 17–4 PH stainless steel: effect of process parameters on mechanical properties, Rapid. Prototyp. J. 29 (5) (2023), https://doi.org/10.1108/RPJ-05-2022-0169.
[36] F. Lavecchia, A. Pellegrini, L.M. Galantucci, Comparative study on the properties of 17-4 PH stainless steel parts made by metal fused filament fabrication process and atomic diffusion additive manufacturing, Rapid. Prototyp. J. 29 (2) (2023), https://doi.org/10.1108/RPJ-12-2021-0350.
[37] D. Cormier, O. Harrysson, H. West, Characterization of H13 steel produced via electron beam melting, Rapid. Prototyp. J. (2004), https://doi.org/10.1108/13552540410512516.
[38] M. Narvan, A. Ghasemi, E. Fereiduni, S. Kendrish, M. Elbestawi, Part deflection and residual stresses in laser powder bed fusion of H13 tool steel, Mater. Des. 204 (2021), https://doi.org/10.1016/j.matdes.2021.109659.
[39] Y. Sun, et al., Thermal and mechanical properties of selective laser melted and heat treated H13 hot work tool steel, Mater. Des. 224 (2022), https://doi.org/10.1016/j.matdes.2022.111295.
[40] G.M. Volpato, U. Tetzlaff, M.C. Fredel, A Comprehensive Literature Review on Laser Powder Bed Fusion of Inconel Superalloys, 2022, https://doi.org/10.1016/j.addma.2022.102871.
[41] R. Wrobel, et al., Influence of wall thickness on microstructure and mechanical properties of thin-walled 316L stainless steel produced by laser powder bed fusion, Mater. Des. 238 (2024) 112652, https://doi.org/10.1016/j.matdes.2024.112652.
[42] M.A. Obeidi, Metal additive manufacturing by laser-powder bed fusion:guidelines for process optimisation, Result. Eng. 15 (2022), https://doi.org/10.1016/j.rineng.2022.100473.
[43] M. Mazur, M. Leary, M. McMillan, J. Elambasseril, M. Brandt, SLM additive manufacture of H13 tool steel with conformal cooling and structural lattices, Rapid. Prototyp. J. 22 (3) (2016), https://doi.org/10.1108/RPJ-06-2014-0075.
[44] M. Armstrong, H. Mehrabi, N. Naveed, An Overview of Modern Metal Additive Manufacturing Technology, 2022, https://doi.org/10.1016/j.jmapro.2022.10.060.
[45] B. Blakey-Milner, et al., Metal additive manufacturing in aerospace: a review, Mater. Des. 209 (2021), https://doi.org/10.1016/j.matdes.2021.110008.
[46] C. Radhika, R. Shanmugam, M. Ramoni, G. BK, A review on additive manufacturing for aerospace application, Mater. Res. Express. 11 (2024).
[47] A.M. Nayeem, M.M.N. Hossain, Usage of Additive Manufacturing in the Automotive Industry: a review, Banglad. J. Multidiscipl. Scientif. Res. 8 (1) (Dec. 2023) 9–20.
[48] S. Cho, S.F. Buchsbaum, M. Biener, J. Jones, M.A. Melia, J.A. Stull, H.R. Colon-Mercado, J. Dwyer, S. Roger Qiu, True active surface area as a key indicator of corrosion behavior in additively manufactured 316L stainless steel, Mater. Des. 237 (Jan. 2024).
[49] H. Selmi, J. Brousseau, G. Caron-Guillemette, S. Goulet, J. Desjardins, C. Belzile, Weldability of 316L parts produced by metal additive manufacturing, J. Manufact. Mater. Process. 7 (2) (2023), https://doi.org/10.3390/jmmp7020071.
[50] K.W. Dalgarno, R.D. Goodridge, Compression testing of layer manufactured metal parts: the RAPTIA compression benchmark, Rapid. Prototyp. J. 10 (4) (2004), https://doi.org/10.1108/13552540410551397.
[51] J. Damon, S. Dietrich, S. Gorantla, U. Popp, B. Okolo, V. Schulze, Process porosity and mechanical performance of fused filament fabricated 316L stainless steel, Rapid. Prototyp. J. 25 (7) (2019), https://doi.org/10.1108/RPJ-01-2019-0002.
[52] P. Lesage, L. Dembinski, R. Lachat, S. Roth, Mechanical characterization of 3D printed samples under vibration: effect of printing orientation and comparison with subtractive manufacturing, Result. Eng. 13 (2022), https://doi.org/10.1016/j.rineng.2022.100372.
[53] L. Zhao, J.G. Santos Macías, A. Dolimont, A. Simar, E. Rivière-Lorphèvre, Comparison of residual stresses obtained by the crack compliance method for parts produced by different metal additive manufacturing techniques and after friction stir processing, Addit. Manuf. 36 (2020), https://doi.org/10.1016/j.addma.2020.101499.
[54] M. Narvan, A. Ghasemi, E. Fereiduni, M. Elbestawi, Laser powder bed fusion of functionally graded bi-materials: role of VC on functionalizing AISI H13 tool steel, Mater. Des. 201 (2021), https://doi.org/10.1016/j.matdes.2021.109503.
[55] J.A. Naranjo, C. Berges, R. Campana, G. Herranz, Rheological and mechanical assessment for formulating hybrid feedstock to be used in MIM & FFF, Result. Eng. 19 (2023), https://doi.org/10.1016/j.rineng.2023.101258.
[56] N. Ahmad, S. Shao, M. Seifi, N. Shamsaei, Additively manufactured IN718 in thin wall and narrow flow channel geometries: effects of post-processing and wall thickness on tensile and fatigue behaviors, Addit. Manuf. 60 (2022), https://doi.org/10.1016/j.addma.2022.103264.
[57] A.E. Medvedev, T. Maconachie, M. Leary, M. Qian, M. Brandt, Perspectives on Additive Manufacturing for Dynamic Impact Applications, 2022, https://doi.org/10.1016/j.matdes.2022.110963.
[58] N.G. March, D.R. Gunasegaram, A.B. Murphy, Evaluation of Computational Homogenization Methods for the Prediction of Mechanical Properties of Additively Manufactured Metal Parts, 2023, https://doi.org/10.1016/j.addma.2023.103415.
[59] A. Mecheter, F.T.M. Kucukvar, A review of conventional versus additive manufacturing for metals: life-cycle environmental and economic analysis, Sustainability 15 (16) (2023) 12229.
[60] S. Li, H. Deng, X. Lan, B. He, X. Li, Z. Wang, Developing cost-effective indirect manufacturing of H13 steel from extrusion-printing to post-processing, Addit. Manuf. 62 (2023), https://doi.org/10.1016/j.addma.2022.103384.
[61] E. Maleki, S. Bagherifard, M. Bandini, M. Guagliano, Surface Post-Treatments for Metal Additive Manufacturing: Progress, Challenges, and Opportunities, 2021, https://doi.org/10.1016/j.addma.2020.101619.
[62] K.D. Traxel, A. Bandyopadhyay, Diamond-reinforced cutting tools using laser-based additive manufacturing, Addit. Manuf. 37 (2021), https://doi.org/10.1016/j.addma.2020.101602.
[63] K.D. Traxel, A. Bandyopadhyay, First demonstration of additive manufacturing of cutting tools using directed energy deposition system: stellite™-based cutting tools, Addit. Manuf. 25 (2019), https://doi.org/10.1016/j.addma.2018.11.019.
[64] Y. Xing, et al., Assessment of self-lubricating coated cutting tools fabricated by laser additive manufacturing technology for friction-reduction, J. Mater. Process. Technol. 318 (2023), https://doi.org/10.1016/j.jmatprotec.2023.118010.
[65] H. Meliani, A. Gilbin, M. Fontaine, M. Assoul, G. Monteil, Surface texturing of cutting inserts for turning of aluminium, Int. J. Adv. Manufact. Technol. (Dec. 2022).
[66] J. Sykora, et al., Additive manufacturing of WC-Co specimens with internal channels, Mater. (Basel) 16 (11) (2023), https://doi.org/10.3390/ma16113907.
[67] H. Shanker, R. Wattal, A comprehensive survey on the cold metal transfer process for additive manufacturing, in: Journal of Physics: Conference Series, 2023, https://doi.org/10.1088/1742-6596/2570/1/012001.
[68] ISO 1832, ISO 1832:2017 Indexable inserts for cutting tools. Designation. International Organization for Standardization (ISO), ISO, 2017.
[69] ISO 6508-1, ISO 6508-1: 2023 metallic materials — Rockwell hardness test Part 1: test method. International Organization for Standardization (ISO), ISO, 2023.
[70] ISO 4287, ISO 4287:2007Geometrical product specifications (GPS) -Surface texture: profile method — Terms, definitions and surface texture parameters. International Organization of Standardization ISO, 2007.
[71] UNE-EN ISO 1302, UNE-EN ISO 1302:2002 Especificación geométrica de productos (GPS). Indicación de la calidad superficial en la documentación técnica de productos. International Organization for Standardization (ISO), 2002.